PHILOSOPHICAL TRANSACTIONS OF THE ROYAL SOCIETY A MATHEMATICAL, PHYSICAL & ENGINEERING SCIENCES

Capsize of ship models in following/quartering waves: physical experiments and nonlinear dynamics

Naoya Umeda and Masami Hamamoto

Phil. Trans. R. Soc. Lond. A 2000 **358**, 1883-1904
doi: 10.1098/rsta.2000.0619

THE ROYAL SOCIETY

Capsize of ship models in following/quartering waves: physical experiments and nonlinear dynamics

By Naoya Umeda and Masami Hamamoto

Department of Naval Architecture and Ocean Engineering, Osaka University, 2-1 Yamada-oka, Suita, Osaka 565-0871, Japan

This paper presents experimental records for capsizing of ship models in following and quartering seas. Recorded capsizes have been classified into four modes: broaching, low cycle resonance, stability loss on a wave crest, and bow diving. Nonlinear dynamics were applied to broaching and low cycle resonance to reveal their qualitative and quantitative characteristics. For other modes, further investigation based on nonlinear dynamics should be encouraged.

Keywords: broaching; bow diving; heteroclinic bifurcation; low cycle resonance; surf-riding

1. Introduction

Capsizing of a ship is a transition from a stable equilibrium point near the upright position to a stable equilibrium point near the upside-down position. This indicates that coexisting stable equilibria are prerequisite for capsizing, and, therefore, a mathematical model used in the study of capsizing should be nonlinear.

Ship capsizing has been regarded as an escape from a potential well (Thompson 1990, 1997). For beam seas it can be modelled with a Duffing-type equation, and, thus, nonlinear dynamics are directly applicable (Wellicome 1975; Thompson 1990). On the other hand, experiments with a radio-controlled ship model showed that a ship is more likely to capsize in following and quartering waves rather than in beam waves (see, for example, Yamakoshi *et al*. 1982). As the encounter period of a ship to beam waves is equal to wave period, a ship with less restoring moment, in other words, long natural roll period, is not likely to be directly synchronized with ocean waves. However, if a ship runs in following and quartering seas, the Doppler effect can make the encounter period longer, up to infinity in principle. Thus, if a ship with lower restoring moment runs in a following or quartering sea with relatively high speed, harmonic resonance cannot be avoided. Furthermore, when the encounter period becomes very long, the surge, sway and yaw motions can be significant, because these motions do not have restoring, in other words, their natural periods can be regarded to be infinite. As a result of coupling among sway, yaw and roll, the roll motion can also be significant. Therefore, capsizing in following and quartering waves with relatively high speeds should be investigated on the basis of a multi-degrees-of-freedom system.

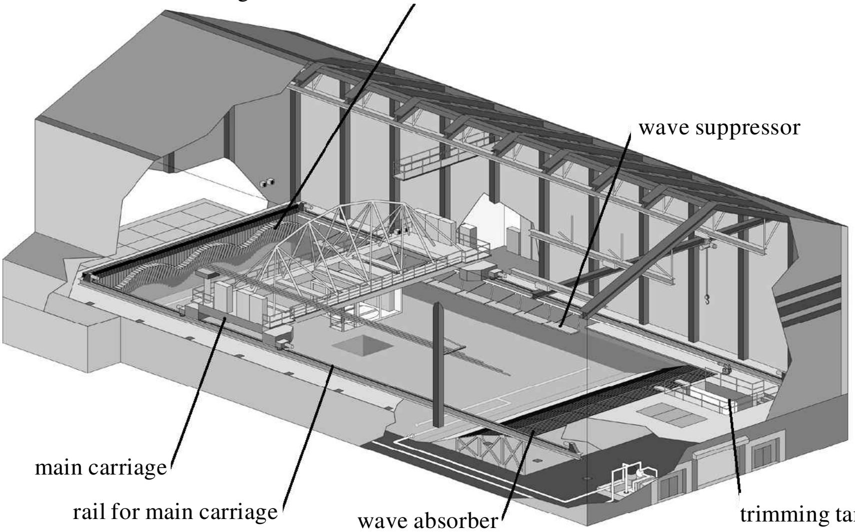

Figure 1. The seakeeping and manoeuvring basin used in the experiments.

The authors have conducted free-running model experiments for several ship models at a seakeeping and manoeuvring basin to examine ship stability criteria and operational guidance (Umeda *et al.* 1995*a*, 1999; Hamamoto *et al.* 1996). These experimental results show that models complying with the existing criteria capsized only in following and quartering seas. The experiments also identified the following modes of capsizing: broaching, low cycle resonance or parametric resonance, bow diving or plough-in, and stability loss on a wave crest. As the classification or definitions for those capsizing modes have been rather vague up till now, the authors attempt to clarify the classification with the help of experimental records, including time-series and photographs taken from digital videotapes. Nonlinear dynamics are useful in estimating the critical condition for these capsizing modes. Since nonlinearity in the system results in dependence on initial values, simple numerical simulations are limited in their ability. Therefore, this paper demonstrates that nonlinear dynamics can, perhaps, be used to qualitatively and quantitatively explain ship capsizes identified with model experiments.

2. Model experiments

The model experiments have been carried out at an indoor seakeeping and manoeuvring basin of the National Research Institute of Fisheries Engineering (NRIFE) in Japan (shown in figure 1). It is 60 m long, 25 m wide and 3.2 m deep. An 80-segment wave maker is equipped to generate regular, long-crested irregular and short-crested irregular waves up to the limit of wave breaking. An X–Y (longitudinally–transversely moving) towing carriage is also available.

The ship models relevant to the present paper are geometrically scaled ones for a 135 GT (gross tonnage) purse seiner, an 80 GT purse seiner, and a 15 000 GT container ship. Their principal dimensions are shown in table 1, and their general arrangements or lines are given in figures 2–4. The ship models were loaded so as to

Table 1. *Principal particulars of the ships*

(The extinction coefficients a and b are defined as $\delta\phi = a\phi_{\mathrm{m}} + b\phi_{\mathrm{m}}^2$, where $\delta\phi$ and ϕ_{m} indicate decrement and mean swing angle of roll decay tests without forward velocity, respectively.)

items	135 GT purse seiner	80 GT purse seiner	container ship
length overall, L_{OA}	43.0 m	36.5 m	162.7 m
length between perpendiculars, L	34.5 m	29.0 m	150.0 m
breadth, B	7.60 m	6.80 m	27.2 m
depth, D	3.07 m	2.60 m	13.5 m
fore draught, d_{f}	2.50 m	2.25 m	8.5 m
mean draught, d_{m}	2.65 m	2.25 m	8.5 m
aft draught, d_{a}	2.80 m	2.25 m	8.5 m
block coefficient, C_{b}	0.597	0.577	0.667
radius of gyration in pitch	$0.242L_{\mathrm{OA}}$	$0.246L_{\mathrm{OA}}$	$0.225L_{\mathrm{OA}}$
longitudinal centre of buoyancy aft of midships	1.31 m	0.42 m	−1.01 m
rudder area ratio, $A_{\mathrm{R}}/Ld_{\mathrm{m}}$	1/26.2	1/20.0	1/44.7
aspect ratio of rudder	1.84	1.68	1.68
time constant of steering gear	0.63 s	0.57 s	1.24 s
rudder gain	1.0	1.0	1.0
propeller diameter	2.60 m	2.18 m	5.04 m
metacentric height, GM	1.00 m	1.36 m	0.15 m
natural roll period	7.4 s	4.5 s	43.4 s
roll extinction coefficient, a	0.044	0.157	0.271
roll extinction coefficient, b	0.030	0.020	0.005
model scale	1/15	1/12.6	1/60

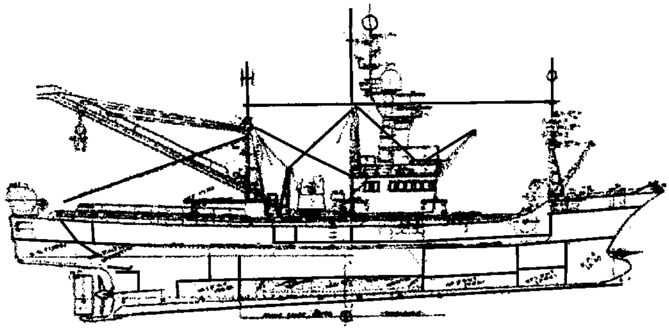

Figure 2. Side view of general arrangement of the 135 GT purse seiner.

comply with the stability and load-line criteria of the International Maritime Organization (IMO) or Japanese government, and their righting-arm curves are shown in figure 5.

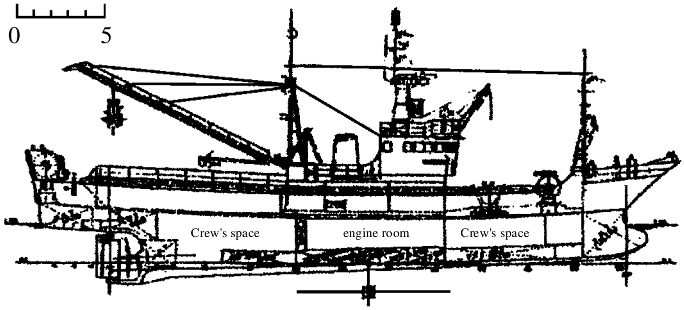

Figure 3. Side view of general arrangement of the 80 GT purse seiner.

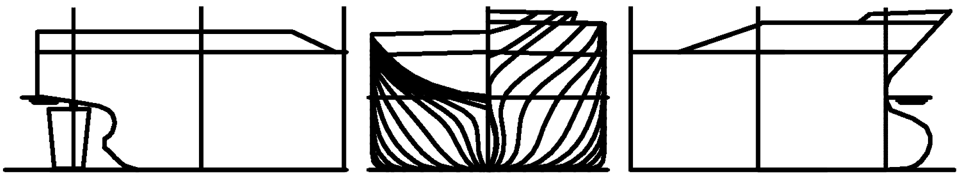

Figure 4. Lines of the container ship.

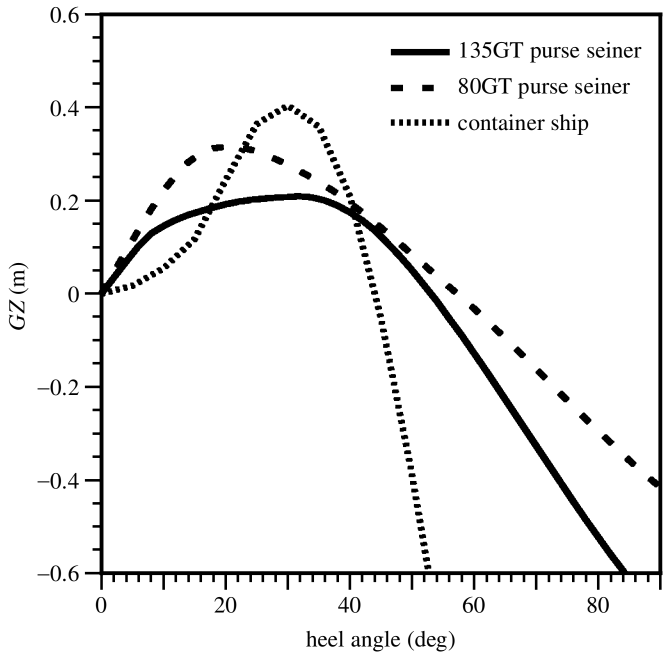

Figure 5. Righting-arm curves for the three ships.

Each ship model was watertight and self-propelled with electric power supplied by solid batteries inside the model. A feedback control system is provided to keep the propeller revolution constant. A fibre gyroscope, a computer and steering gear were also equipped, and a proportional autopilot for course keeping was simulated within the onboard computer by using the yaw angle obtained from the gyroscope. The roll angle, pitch angle, yaw angle, rudder angle and propeller revolution were recorded

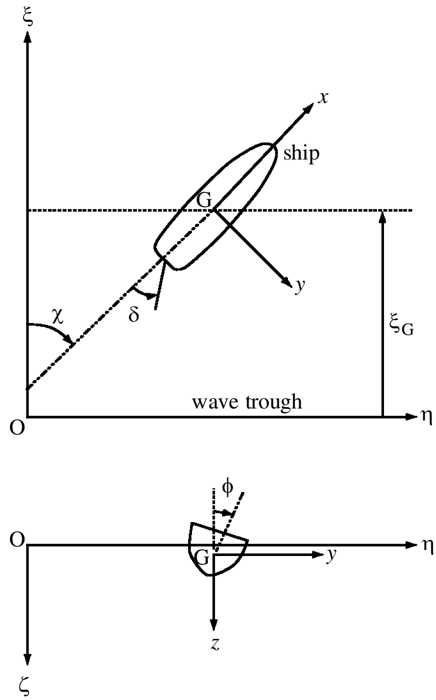

Figure 6. Coordinate systems.

by the onboard computer. As shown in figure 6, two coordinate systems were used for the reference to their motions: one is the wave fixed system with origin at a wave trough, ξ-axis in the direction of wave travel; the other is the body fixed system with origin at the centre of ship gravity, the x-axis pointing towards the bow, the y-axis to starboard, and the z-axis downwards. That is, positive pitch is bow up, positive roll results in downward movement of the starboard side, positive yaw is to starboard from the wave direction, and positive rudder angle induces positive yaw in calm water.

The experimental procedure for following and quartering waves is as follows. First, the model is kept near the wave maker without propeller revolution. Next, the wave maker starts to generate regular waves. After a generated water wave train propagates enough, a radio operator immediately increases the propeller revolution up to the specified one and makes the autopilot active for the specified course. Then the model automatically runs in following and quartering seas to keep the specified propeller revolution and autopilot course. When the model approaches the side wall or the wave-absorbing beach, the automatic control is interrupted by the radio operator and the propeller is reversed to avoid collision. Throughout this paper, the specific propeller revolution is indicated by the nominal Froude number, F_{n}, which is the Froude number when the ship runs in otherwise calm water with that propeller revolution.

3. Capsizing due to broaching

Broaching is a phenomenon in which a ship cannot keep a constant course despite the maximum steering effort of her helmsman. This phenomenon is likely to occur when a

PHILOSOPHICAL TRANSACTIONS OF THE ROYAL SOCIETY A MATHEMATICAL, PHYSICAL & ENGINEERING SCIENCES

ship is surf-ridden on a wave downslope. When the corresponding calm-water velocity is smaller than the wave celerity, the ship may be accelerated up to the wave celerity and be forced to run with the wave downslope near the wave trough because of the positive wave-induced surge force. This is known as surf-riding, and has already been explained as a kind of nonlinear phenomenon (Ananiev 1966; Makov 1969; Umeda & Kohyama 1990). On the downslope near the wave trough, the wave-induced yaw moment, which forces the ship to turn, increases when the heading angle increases. Thus, the ship situated on the downslope near the trough is directionally unstable (Davidson 1948). Even though the helmsman applies the maximum opposite rudder angles, a violent yaw motion can occur in the event of insufficient rudder ability. The centrifugal force due to this violent yaw motion may make the ship capsize (Motora *et al*. 1982).

In the model experiments carried out by the authors, capsizing due to broaching was often observed for the 135 GT purse seiner complying with the intact stability code of the IMO. Examples of the time-series and photographs taken from a digital videotape are shown in figures 7 and 8, respectively. Here, the wave steepness is 1/9.3 and the ratio of wave length to ship length is 1.413. The nominal Froude number is 0.43 and the autopilot course is -10° from the wave direction. As shown in photograph 1 of figure 8, the model was initially overtaken by the waves. It was then captured by a wave remaining on the downslope, and, thus, surf-riding was realized (photograph 2). During this stage, the pitch angle tended to a negative constant value. While on the downslope, the yaw angle started to increase to port (photograph 3), and the rudder controlled by the autopilot responded to prevent this yaw motion. However, despite the hard-starboard, the increase in yaw continued (photographs 4 and 5). Here, the centrifugal force due to large yaw rate, wave-induced force and rudder force forced the model to roll towards starboard (photograph 6). As a result, the model capsized in this direction (photographs 7–9). Thus, this is a typical example of a capsize due to broaching.

To investigate broaching with nonlinear dynamics, it is necessary to establish a mathematical model for it. Generally, three-dimensional movement of a rigid body has six degrees of freedom, but restoring in heave and pitch are dominant in this case. In other words, the natural frequencies of heave and pitch are very high. Hence, when the ship runs with relatively high speed in following and quartering seas, the encounter frequency is much smaller than those natural frequencies. Therefore, heave and pitch can be reasonably approximated by simply tracing their static equilibria (Matsuda *et al*. 1997).

This outcome indicates that a surge–sway–yaw–roll mathematical model is suitable for investigating broaching if we use coefficients for a ship free in heave and pitch. Here, we use a modular manoeuvring mathematical model incorporated with wave effects, because hydrodynamic forces at low frequency mainly consist of the lift component and the wave making component is negligible (Umeda & Renilson 1992; Umeda 1999). Based on this mathematical model, the state vector, $\boldsymbol{x}$, and control vector, $\boldsymbol{b}$, of this system are defined, respectively, as

$$\boldsymbol{x} = \{\xi_G/\lambda, u, v, \chi, r, \phi, p, \delta\}^T, \tag{3.1}$$

$$\boldsymbol{b} = \{n, \chi_c\}^T, \tag{3.2}$$

where ξ_G is the longitudinal position of the centre of gravity of the ship from a wave trough, λ is the wavelength, u is the surge velocity, v is the sway velocity, χ is the

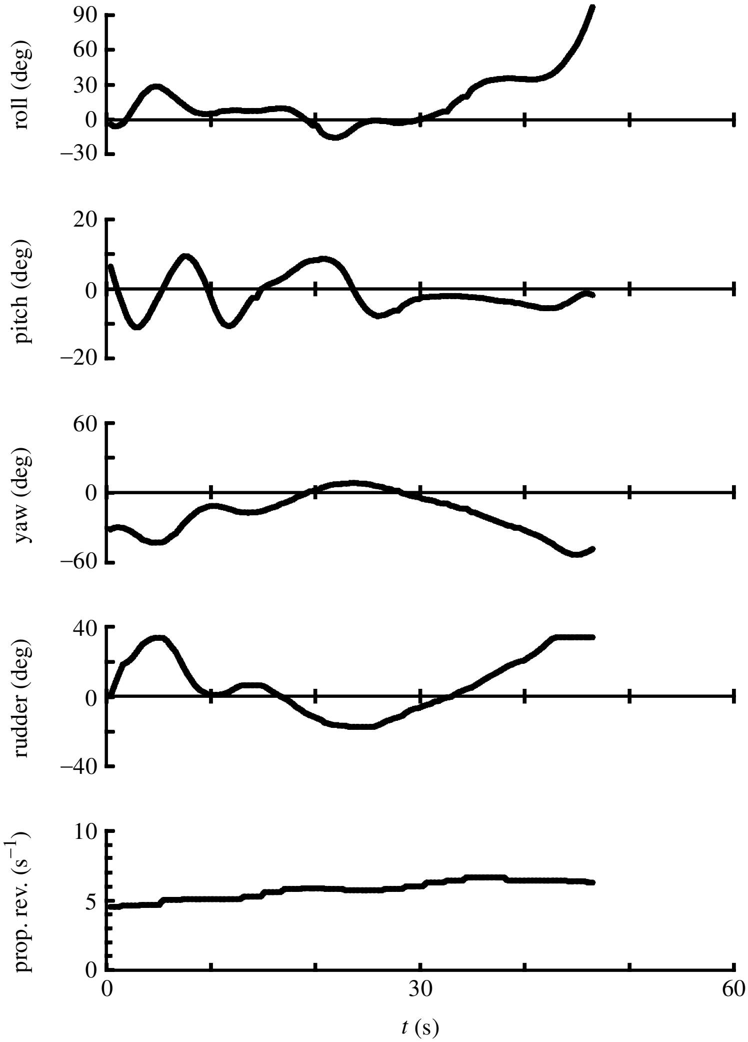

Figure 7. Time-series of capsize due to broaching for the 135 GT purse seiner with wave steepness of 1/9.3, the wavelength-to-ship length ratio of 1.413, autopilot course of $-10°$ and nominal Froude number of 0.43 (Umeda *et al.* 1999).

heading angle, r is the yaw rate, ϕ is the roll angle, p is the roll rate, δ is the rudder angle, n is the propeller revolution, and χ_c is the autopilot course.

The dynamical system can be represented by the following state equation:

$$\dot{\boldsymbol{x}} = \boldsymbol{F}(\boldsymbol{x}; \boldsymbol{b}), \tag{3.3}$$

where $\boldsymbol{F}$ consists of resistance, propulsion force, virtual inertia, manoeuvring forces, wave forces and rudder response (Umeda & Vassalos 1996). Dots denote differentiation with respect to time. Since the external forces are functions of the surge displacement but not of time, this equation is nonlinear and autonomous. The wave forces and moments can be predicted to be the sum of the Froude–Krylov components and the hydrodynamic lift due to wave particle velocity by a slender body theory

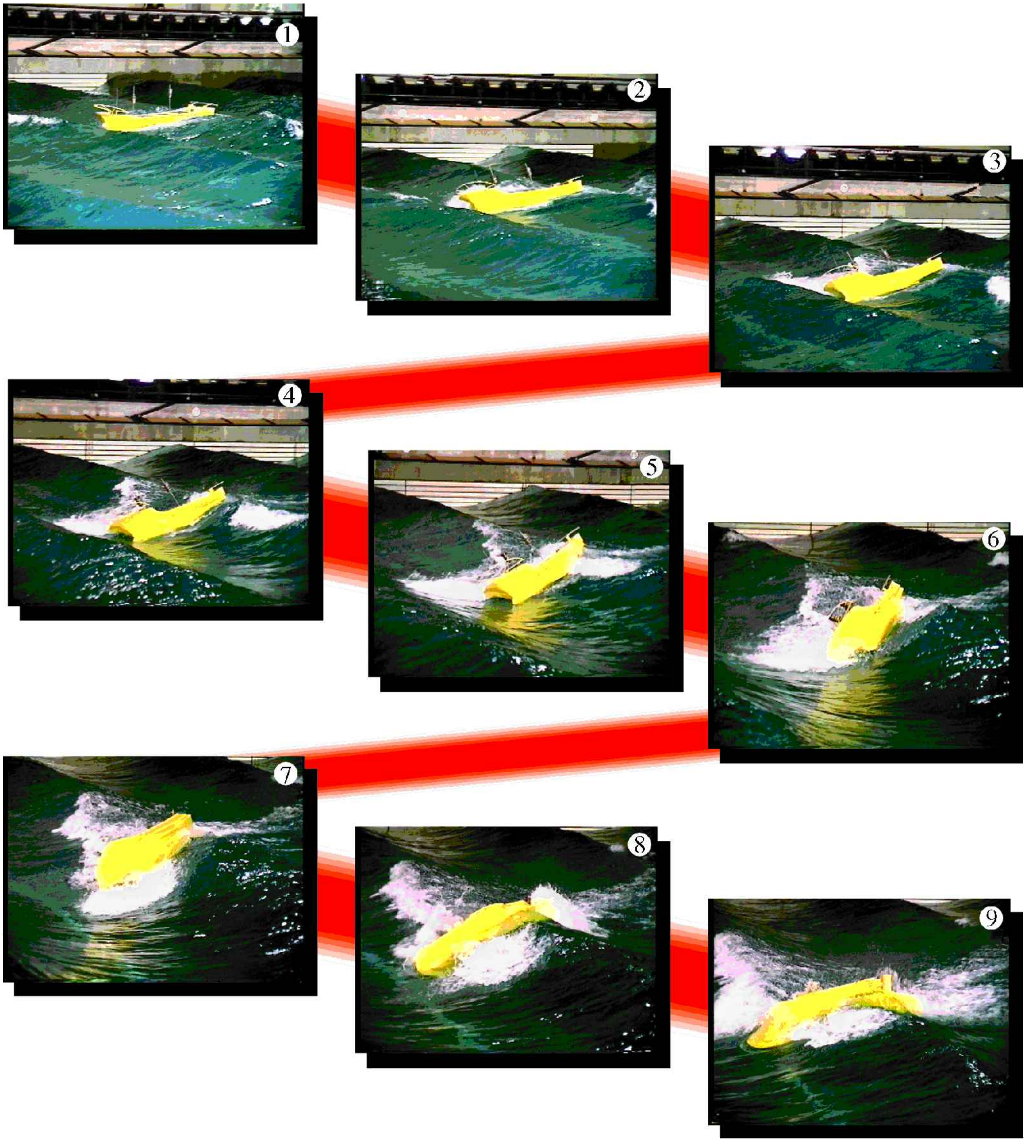

Figure 8. Photographs of capsize due to broaching for the 135 GT purse seiner with wave steepness of 1/9.3, the wavelength-to-ship length ratio of 1.413, autopilot course of −10° and nominal Froude number of 0.43.

with reasonable accuracy (Umeda *et al.* 1995*b*). As they are major steady-states of this system, fixed points and periodic orbits have been focused on here. First, the fixed points, $\bar{\boldsymbol{x}}$, are obtained by solving the following equation:

$$\boldsymbol{F}(\bar{\boldsymbol{x}}; \boldsymbol{b}) = \boldsymbol{0}. \tag{3.4}$$

If a solution exists, the ship will be in a surf-riding equilibrium on a wave with a drift angle, heading angle, heel angle and rudder angle. The stability of this fixed point can be examined by calculating eigenvalues of locally linearized equations at the fixed point (Umeda & Renilson 1992; Spyrou 1995).

PHILOSOPHICAL TRANSACTIONS OF THE ROYAL SOCIETY A MATHEMATICAL, PHYSICAL & ENGINEERING SCIENCES

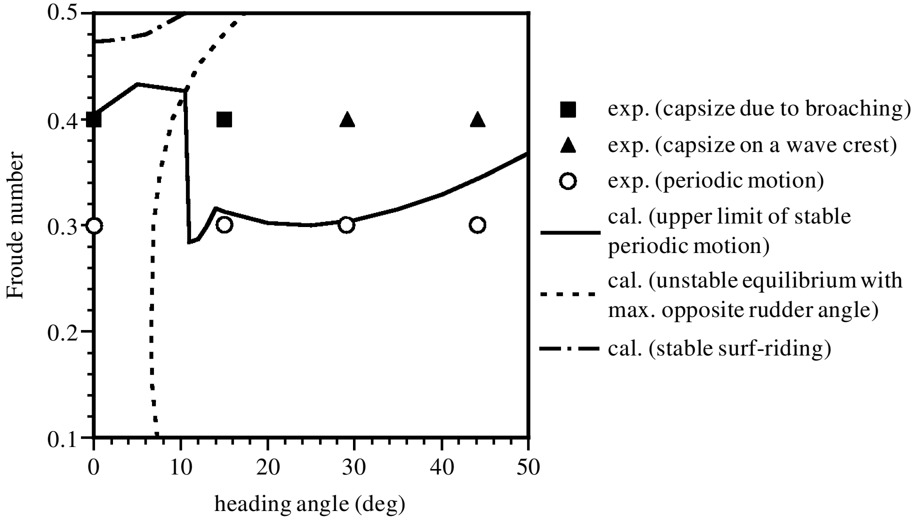

Figure 9. Comparison between the results of the model experiments and the critical conditions for the fixed points and periodic orbits estimated by the theoretical prediction methods for the 135 GT purse seiner with wave steepness of 1/15 and wavelength-to-ship length ratio of 1.5 (Umeda *et al*. 1997).

For investigating the periodic orbits, namely periodic ship motions, the mathematical model has been converted to that based on a coordinate system moving with the average ship velocity and then the averaging method has been applied. Since the averaging theorem indicates that the existence and stability of the fixed point of the averaged equation correspond to those of the periodic orbit of the original equation, the periodic orbits and their stability can be calculated using this procedure (Umeda & Vassalos 1996).

The comparison between the results of the model experiments and the critical conditions for the fixed points and periodic orbits estimated by the above procedures is shown in figure 9. When the nominal Froude number is low, a stable periodic orbit theoretically exists, and this was experimentally confirmed. Then, when the nominal Froude number increases up to a certain value, this periodic orbit may become unstable. On the other hand, a fixed point, which corresponds to surf-riding, exists for smaller autopilot course angle. While it can be stable for high Froude number, i.e. in the region above the dashed–dotted line, it is generally a saddle in the region surrounded by the dashed–dotted line, the ordinate and the dotted line, for any possible rudder angle. In the region where both the periodic orbit and the fixed point are unstable, the ship can be attracted by the saddle and then repelled with a violent yaw motion. As the calculated result indicates that this motion cannot be avoided, even with immediate application of the maximum opposite rudder, i.e. the bang–bang control, broaching can occur. In the experiment, capsizing due to broaching was generally observed near the unstable fixed point with maximum opposite rudder being applied in the region where the periodic orbit was unstable. Thus, this approximated analysis of nonlinear dynamics showed a reasonably good comparison with model experiments for the critical condition of capsizing due to broaching (Umeda *et al*. 1997).

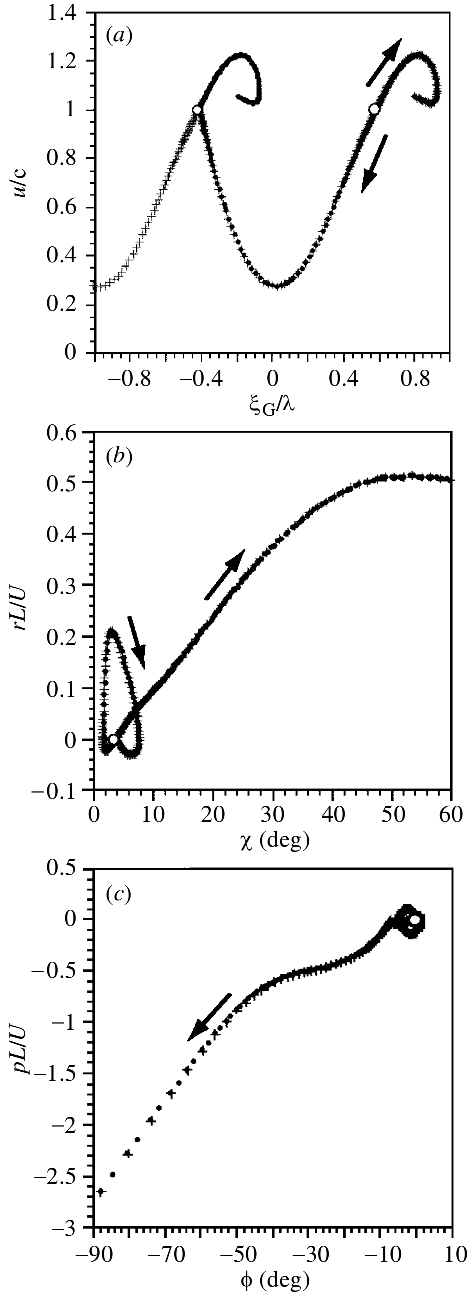

Figure 10. Unstable invariant manifold of the fixed point near the wave crest for the 135 GT purse seiner with wave steepness of 1/9.2, wavelength-to-ship length ratio of 1.5, autopilot course of −10°. Here the small filled circles and the crosses indicate the manifold for the nominal Froude numbers of 0.3248 and 0.3247, respectively. The open circle represents the fixed point near the wave crest and c denotes the waves' celerity; U is the ship's forward velocity. (a) The projection onto the surge-displacement–surge-velocity plane. (b) The projection onto the yaw–yaw rate plane. (c) The projection onto the roll–roll rate plane.

To investigate broaching more directly, invariant manifolds of unstable fixed point are examined. Since the fixed point is generally a saddle of index one, its unstable invariant manifold or outset is one dimensional. As is well known, the unstable manifold can be obtained approximately by numerically integrating the state equation from the fixed point with a small perturbation in the positive or negative direction of the eigenvector of the eigenvalue having a positive real part. In the case of lower nominal Froude number, the unstable manifold from a fixed point near the wave crest towards the upslope tends to a periodic orbit. However, when the nominal Froude number is higher than a certain value, the unstable manifold from the fixed point near the wave crest does not do this. Figure 10 shows the unstable manifolds for just above and just below this threshold. For a nominal Froude number of 0.3247, the unstable manifold of a fixed point near the wave crest towards the upslope approaches a fixed point near the next wave crest and then tends to a periodic orbit. By contrast, for a nominal Froude number of 0.3248, the unstable manifold approaches the fixed point near the next wave crest and is then captured on the wave downslope. At the same time, the heading angle violently increases to starboard, despite the application of the proportional autopilot, and the roll angle increases to port. Finally, the roll angle exceeds 90°, which can be regarded as capsizing given the restoring moment presented in figure 5. Thus, the calculation is terminated. This behaviour corresponds to the capsizing due to broaching that was observed in the model experiment. We can presume that between these two nominal Froude numbers there is a certain nominal Froude number whose unstable manifold of the saddle tends to a different saddle. This is a 'heteroclinic connection'. Thus, the heteroclinic bifurcation indicates the critical condition for capsizing due to broaching. This fact was also suggested by numerical experiment by Spyrou (1997). Further discussion with comparisons of the unstable manifold and numerical experiments is published separately (Umeda 1999).

4. Capsizing due to low cycle resonance

When the ship centre exists on a crest of waves whose length is comparable with the ship length, relative wave elevations at bow and stern become lower. Because of requirements from seakeeping and propulsion, bow and stern sections have flare and the midship section is wall-sided at the water plane. Thus, when the ship centre exists on the wave crest, the effective water plane breadth of the ship decreases, and, as a result, her restoring moment decreases. Conversely, the restoring moment increases when the ship centre is situated on the wave trough. Thus, when the ship runs in longitudinal waves, her restoring moment periodically changes with time. As a result, if the encounter period is a multiple of half of the natural roll period, the roll motion develops with a period equal to the natural roll period. This is commonly known as the parametric resonance. The regime of parametric resonance in which the encounter period is half of the natural roll period is often called low cycle resonance; it is the most significant regime and may easily lead to capsizing.

In our experiments, capsize due to low cycle resonance was observed when a container ship model complying with the IMO intact stability code runs in following waves. An example of the measured time-series in long-crested irregular waves is shown in figure 11, and an example of photographs in regular waves is given in figure 12. In this case, as the model was overtaken by the waves, the zero upcrossing of the pitch angle indicates a wave crest at the ship centre, as discussed above. When-

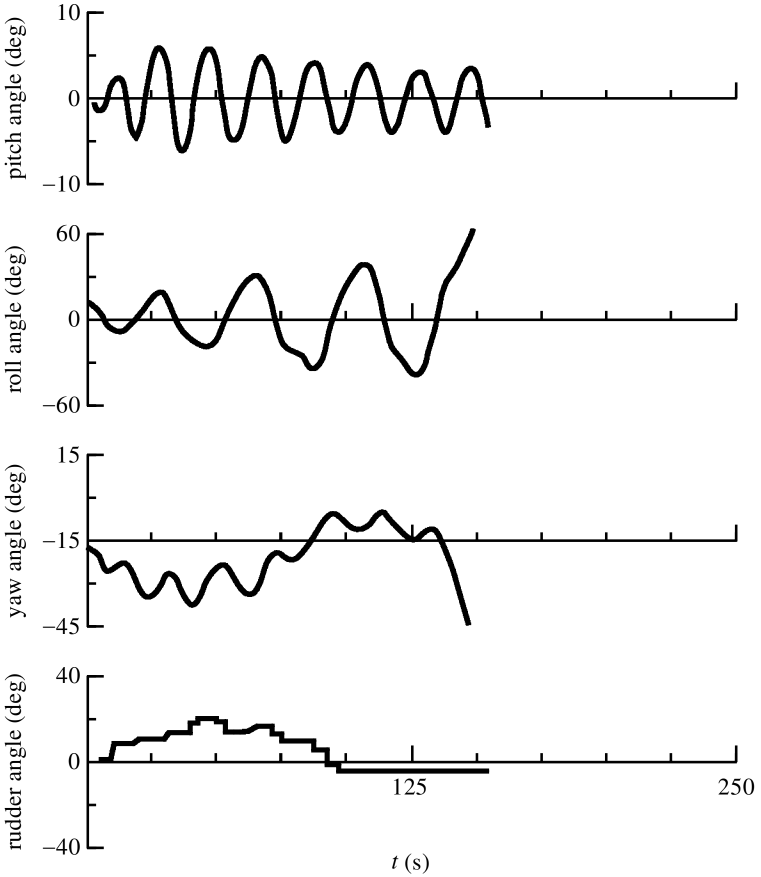

Figure 11. Time-series of capsizing due to low cycle resonance for the contained ship in long-crested irregular waves with the significant wave height of 13.3 m, mean wave period of 10.9 s, nominal Froude number of 0.23 and autopilot course of $-15°$ (Umeda *et al.* 1995*a*).

PHILOSOPHICAL TRANSACTIONS OF THE ROYAL SOCIETY A MATHEMATICAL, PHYSICAL & ENGINEERING SCIENCES

ever the ship centre meets a wave crest, the ship rolls to starboard and port by turns. Thus, the roll period is twice as long as the pitch period corresponding to the encounter period, and coincides with the roll natural period. This aspect of low cycle resonance can be found also in the photographs of figure 12. The model rolled to port at the wave crest (photograph 1) and then rolled to starboard at the next wave crest (photograph 2). At the third wave crest it rolled to port (photograph 3) and it rolled to starboard at the fourth wave crest (photograph 4). At the fifth wave crest it rolled to port again (photograph 5). The model returned to upright at the following wave trough (photograph 6) and rolled significantly to starboard at the sixth wave crest (photograph 7). This excessive roll could not be stabilized at the following wave trough (photograph 8) and, finally, the model capsized (photograph 9).

While the experimental records of low cycle resonance show some coupled motions, it has already been established that the principal nature of parametric resonance can be explained even with an uncoupled roll model with the change of restoring moment taken into account (Kerwin 1955). Although applicability of a coupled model to the low cycle resonance is a research topic for the future, this paper uses the following

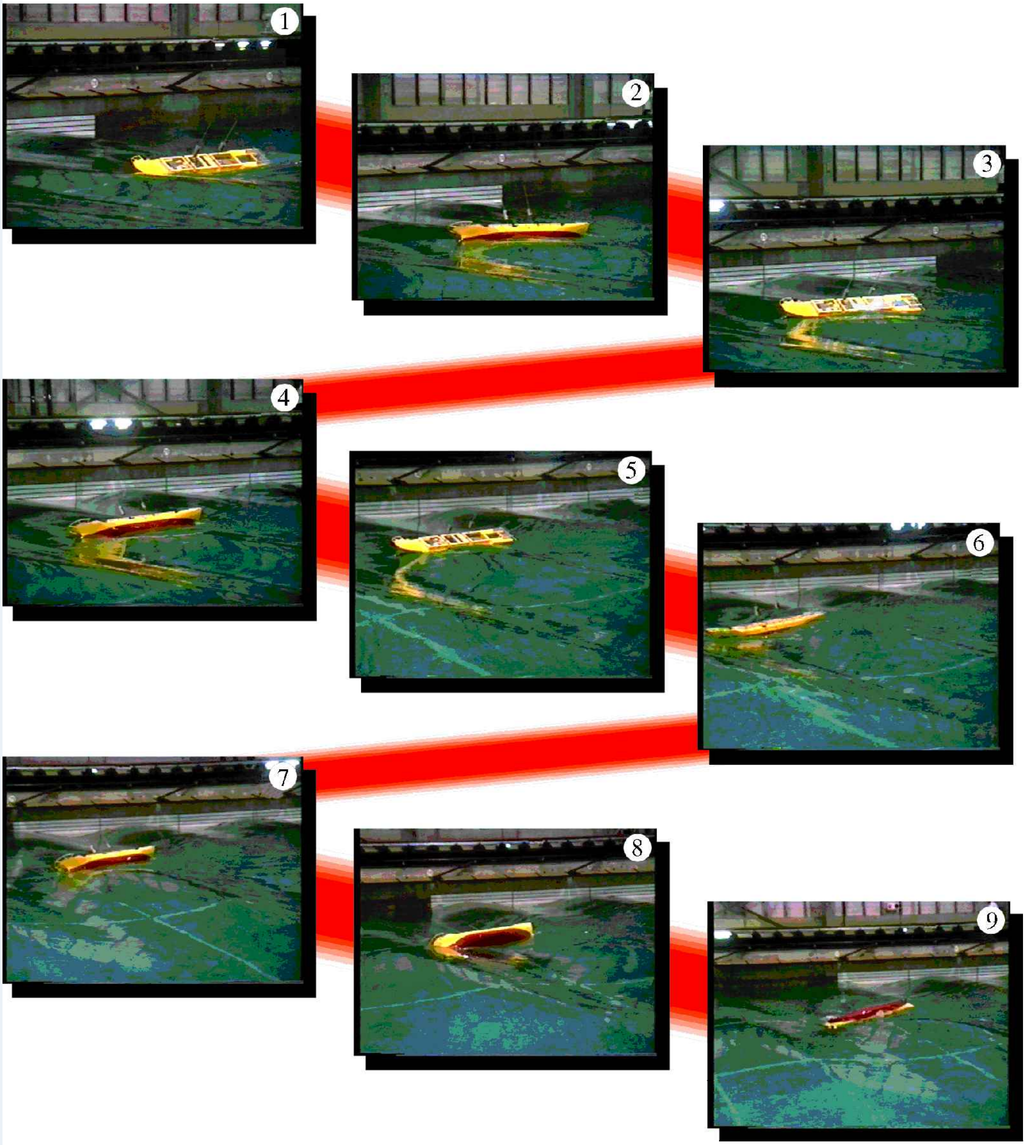

Figure 12. Photographs of capsizing due to low cycle resonance for the container ship in regular waves with the significant wave height of 13.3 m, mean wave steepness of 1/25, wavelength-to-ship length ratio of 1.5, the nominal Froude number of 0.23 and autopilot course of −15°.

uncoupled, but nonlinear, roll model to explain the qualitative nature observed in the experiments:

$$\ddot{\phi} + 2\alpha\dot{\phi} + \omega_\phi^2(1 + M\cos\omega_{\mathrm{e}}t)\phi + \omega_\phi^2\beta\phi^3 = \zeta_{\mathrm{w}}\gamma k\omega_\phi^2\sin\chi\sin\omega_{\mathrm{e}}t, \qquad (4.1)$$

where ϕ is the roll angle, α is the linearized roll damping coefficient, ω_ϕ is the natural roll frequency, M is the amplitude of righting-arm variation as a function of wave amplitude and heading angle, β is the nonlinear righting-arm coefficient, γ is

PHILOSOPHICAL TRANSACTIONS OF THE ROYAL SOCIETY A MATHEMATICAL, PHYSICAL & ENGINEERING SCIENCES

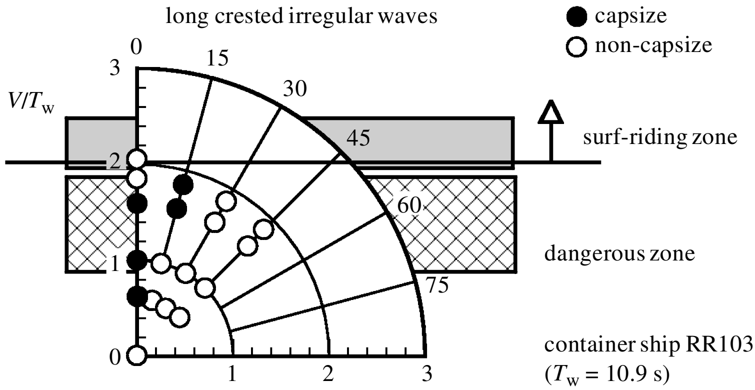

Figure 13. Experimental results for the container ship in long-crested irregular seas with the significant wave height of 13.3 m and mean wave period of 10.9 s. Here V indicates the ship speed in knots and T_w is the mean wave period in seconds. All capsizes marked here are those due to low cycle resonance. The shaded areas are provided by a draft operational guidance (Umeda *et al.* 1995*a*).

the effective wave slope coefficient, k is the wavenumber, ω_e is the encounter wave frequency, and ζ_w is the wave amplitude. Here, the right-hand side of equation (4.1) represents the wave-exciting roll moment. This nonlinear equation of motion can have several solutions. However, the low cycle resonance was observed in the model run shown in figure 12. Thus, it is appropriate here to assume the low cycle resonance corresponding to the condition $\omega_e = 2\hat{\omega}$, where the solution has the form

$$\phi = A\cos(\hat{\omega}t - \varepsilon). \tag{4.2}$$

As discussed in the appendix, the averaged equations are obtained as follows:

$$\dot{A} = -\alpha - \frac{\omega_\phi^2}{4\hat{\omega}} MA\sin 2\varepsilon, \tag{4.3}$$

$$\dot{\varepsilon} = \tfrac{1}{2}\hat{\omega} - \frac{1}{2}\frac{\omega_\phi^2}{\hat{\omega}}(1 + \tfrac{3}{4}\beta A^2) - \frac{1}{4}\frac{\omega_\phi^2}{\hat{\omega}} M\cos 2\varepsilon. \tag{4.4}$$

If we substitute zero into the left-hand sides of the above equations, steady states of low cycle resonance can be obtained as their solutions. If we locally linearize these equations at their solutions, stability of the low cycle resonance can be examined. Hence, these equations indicate that the existence of low cycle resonance and its stability do not depend on the exciting term. Thus, the effect of heading angle on low cycle resonance appears only in the magnitude of change of restoring moment due to waves. Since the change of restoring moment in pure following waves, $\chi = 0$, is almost the largest, capsize due to low cycle resonance is most likely to occur when the heading angle is zero, and danger decreases with increasing heading angle. This theoretical conclusion was qualitatively validated by our model experiments, as shown in figure 13 (Umeda *et al.* 1995*a*). Further detailed analysis of the simplified model given in equation (4.1), including bifurcation diagrams, was carried out by Taguchi & Kan (1992). They showed that the boundary between capsizing and non-capsizing, which is obtained by repeating numerical time integration of the model equation from a grid of starts, is fractal. The authors also obtained a non-smooth

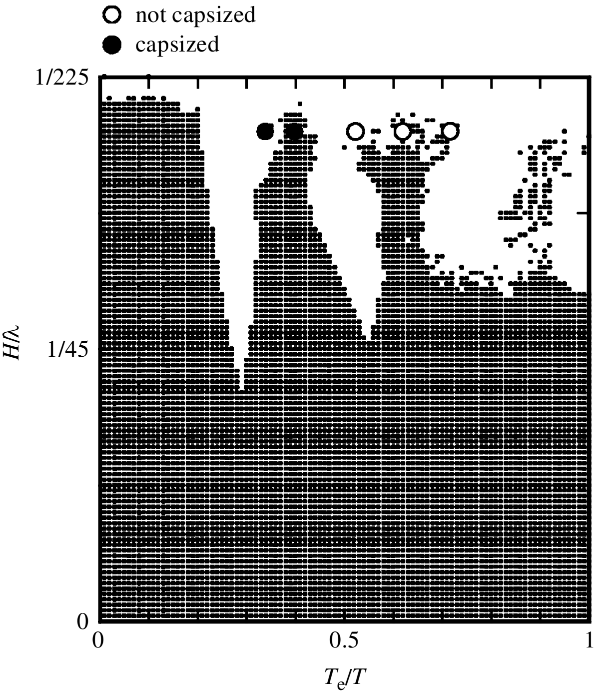

Figure 14. Capsizing boundary obtained by the mathematical model with the change of restoring moment due to waves with the wavelength-to-ship length ratio of 1.5 and relevant experimental results. The abscissa is the ratio of the encounter period to the natural roll period and the ordinate is the wave steepness (Hamamoto *et al*. 1995).

capsizing boundary from the mathematical model with exact form of righting-arm variation and reasonable comparison with their own model experiments, as shown in figure 14 (Hamamoto *et al*. 1995). Here, the dark areas indicate non-capsizing regions obtained by the mathematical model. The empty and filled circles indicate non-capsizing and capsizing observed in physical model experiments, respectively.

5. Capsizing due to stability loss on a wave crest

Our model experiments for the purse seiners showed two other capsizing modes, which have not yet been fully investigated from the viewpoint of nonlinear dynamics. One of them can be found for the 80 GT purse seiner in the autopilot course range between −30 and −60° (Umeda *et al*. 1999). Examples of the time-series and photographs are given in figures 15 and 16. Here, the trapped water on deck induced a leeward heel angle and the roll angle increased whenever a wave crest passed the midship, because the restoring moment decreases when the ship centre is situated on a wave crest. Finally, the model capsized on a wave crest. During this sequence, significant coupled motion of sway, yaw and roll was observed. As shown in the photographs of figure 16, the model significantly yawed to port on a wave downslope (photograph 1) and it yawed to starboard on the next upslope (photograph 2). It then yawed insignificantly to port on the next downslope (photograph 3) and yawed to starboard on the next upslope (photograph 4). It significantly yawed to port on

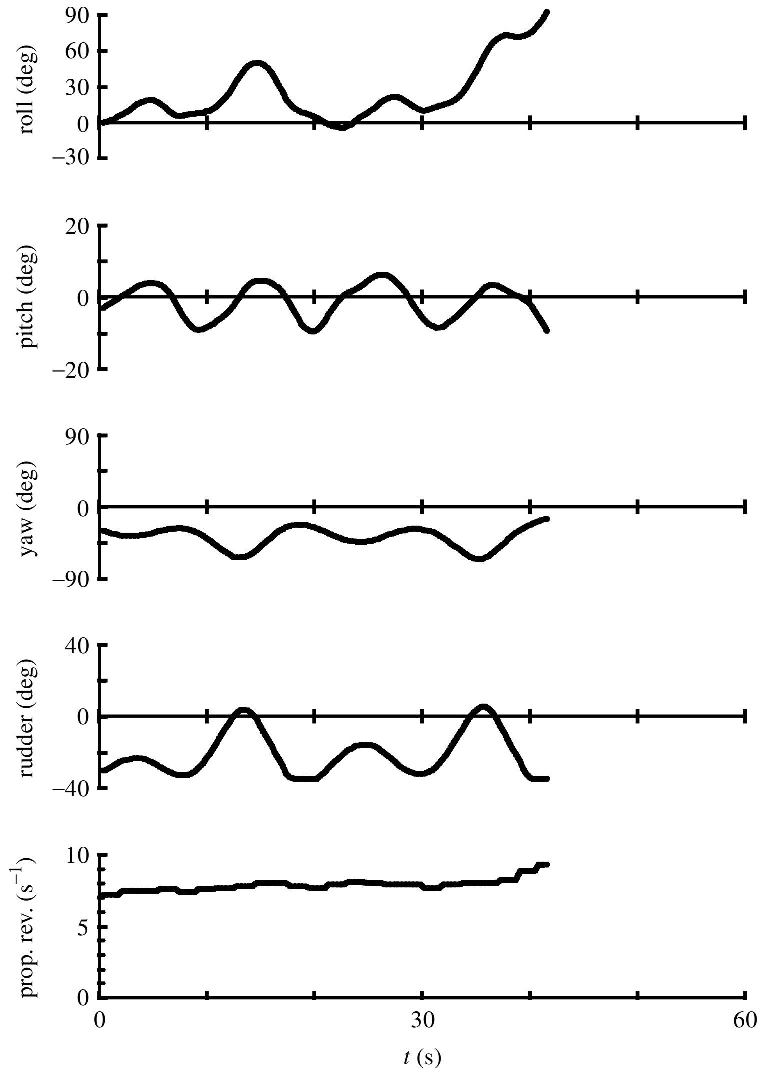

Figure 15. Time-series of capsizing due to stability loss on a wave crest for the 80 GT purse seiner with wave steepness of 1/8.8, wavelength-to-ship length ratio of 1.408, autopilot course of −60° and nominal Froude number of 0.43 (Umeda *et al.* 1999).

the next downslope (photograph 6) and then it rolled largely to starboard on the following wave crest (photograph 7). Finally, the model capsized (photographs 8 and 9).

If we focus on the final stage, this capsizing can be categorized as the capsizing due to stability loss on a wave crest, in which the reduced restoring moment on the wave crest cannot counteract the heeling moment because of trapped water. It is not wholly appropriate to use the phrase 'pure loss of stability' here, because there is significant coupled motion. Pure loss of stability has been regarded as capsizing due to loss of static balance on a wave crest in a following way (Oakley *et al.* 1974). Due to surging, a ship spends more time on a wave crest and less time on a wave trough.

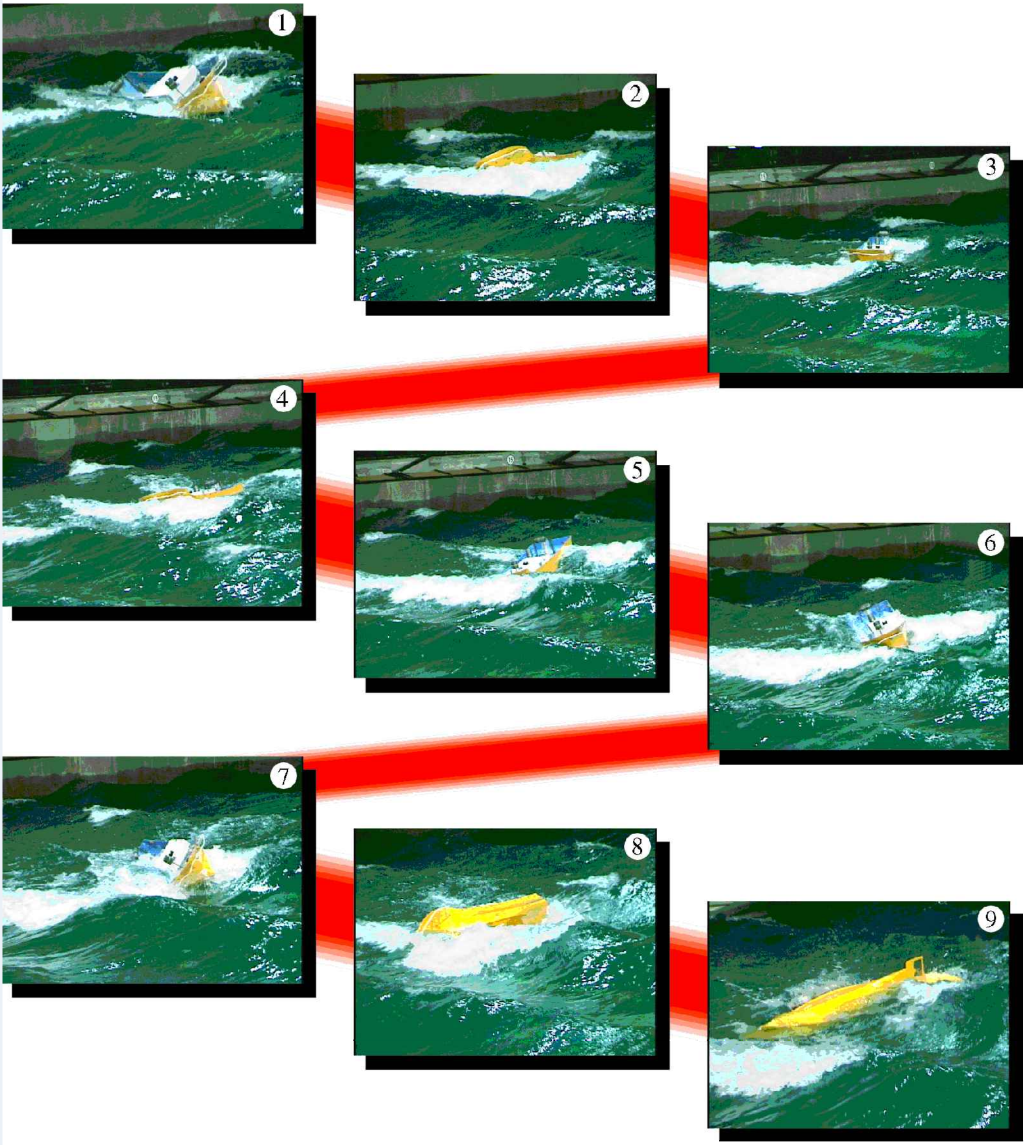

Figure 16. Photographs of capsizing due to stability loss on a wave crest for the 80 GT purse seiner with wave steepness of 1/8.8, wavelength-to-ship length ratio of 1.408, autopilot course of −60° and nominal Froude number of 0.43.

PHILOSOPHICAL TRANSACTIONS OF THE ROYAL SOCIETY A MATHEMATICAL, PHYSICAL & ENGINEERING SCIENCES

If her restoring moment significantly decreases on a wave crest and her heading angle is nearly zero, roll angle can increase exponentially. This typical behaviour of capsizing was not found in our experiments. The capsizing mode observed here may be regarded as the loss of dynamic stability of a coupled periodic motion. Spyrou (1997) pointed out numerically that instability of periodic motions, including the flip-and-fold bifurcation, can be related to cumulative broaching. In fact, in this present example, the yaw period is twice as long as the pitch period. Further investigation using nonlinear dynamics is desirable in order to explain the capsizing observed here.

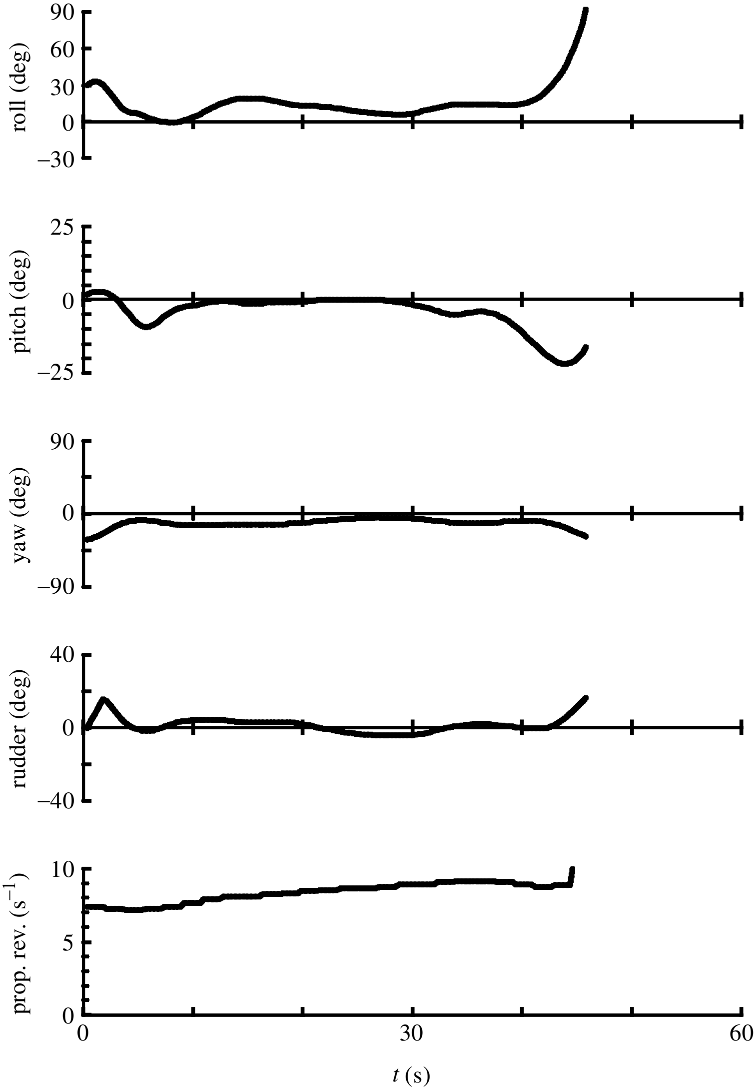

Figure 17. Time-series of capsizing due to plough-in for the 80 GT purse seiner with wave steepness of 1/8.8, wavelength-to-ship length ratio of 1.408, autopilot course of $-10°$ and nominal Froude number of 0.46 (Umeda *et al.* 1999).

6. Capsizing due to bow diving or plough-in

Another type of capsizing that nonlinear dynamics has not yet fully treated was found when the 80 GT purse seiner model ran with a nominal Froude number of 0.46 and the autopilot course of $-10°$. The time-series and photographs for this situation are given in figures 17 and 18. Firstly, the almost constant and zero pitch angle indicates that the model suffered surf-riding on a wave trough (photograph 3 of figure 18). The bow then dived into the upslope (photographs 4 and 5). When the pitch angle reached *ca.* $-20°$, the water plane area decreased due to exposure of the stern (photograph 7). This decrease in the water plane area resulted in the reduction of the righting lever, and, finally, the model capsized (photograph 9). This mode of capsizing is known for a high-speed craft as bow diving or plough-in (Dand 1996). Here, the principal trigger of this capsizing was high nominal Froude number, in other words, large propeller thrust. Because of this, the stable equilibrium in longitudinal force shifted from the downslope to a wave trough, where the bow is likely to submerge (Umeda 1983). Although this nominal Froude number is higher than the actual one, future improvement for increasing forward speed would induce this type of danger. Numerical simulation of this phenomenon, including a phase-plane analysis of surge behaviour, was reported with a surge–heave–pitch mathematical model (Renilson & Anderson 1997). Further investigation based on nonlinear dynamics should be encouraged in order to identify and explore the phenomenon observed in the experiments.

7. Conclusions

Several capsizing modes for a ship in following and quartering seas have been realized in model experiments at the seakeeping and manoeuvring basin, and categorized with the help of time-series and sets of photographs taken from videotapes. For capsizing due to broaching, critical conditions estimated with nonlinear dynamics are compatible with experimental results, and nonlinear dynamics revealed the relationship with a heteroclinic bifurcation. For capsizing due to low cycle resonance, nonlinear dynamics explained the qualitative nature of the capsizing observed in the experiments. For capsizing due to stability loss on a wave crest and bow diving, the authors made some suggestions for further investigation based on nonlinear dynamics.

This paper is based on several research projects funded by the Ministry of Agriculture, Forestry and Fisheries of Japan, the Shipbuilding Research Association of Japan, the Fishing Boat Association of Japan, and the Ministry of Education, Science, Sports and Culture of Japan. The authors acknowledge their support. The authors thank Mr A. Matsuda, Mr S. Suzuki, and other colleagues at the NRIFE, and Mr W. Sera of Kobe University of Mercantile Marine for their assistance in model testing. Special appreciation is due to Mr H. Takahashi of the NRIFE for preparing photographs from the digital videotapes of experiments.

Appendix A.

Equations (4.3) and (4.4) are derived using the following procedure, which was applied to a roll model without a parametric restoring term (Sadakane 1986). If we assume equation (4.2) is a solution of equation (4.1), the roll rate is obtained as follows:

$$\dot{\phi} = -A\hat{\omega}\sin(\hat{\omega}t - \varepsilon). \tag{A 1}$$

Thus, the following two formulae are easily found:

$$\phi^2 + \left(\frac{\dot{\phi}}{\hat{\omega}}\right)^2 = A^2; \tag{A 2}$$

$$\tan(\hat{\omega}t - \varepsilon) = -\frac{1}{\hat{\omega}}\left(\frac{\dot{\phi}}{\phi}\right). \tag{A 3}$$

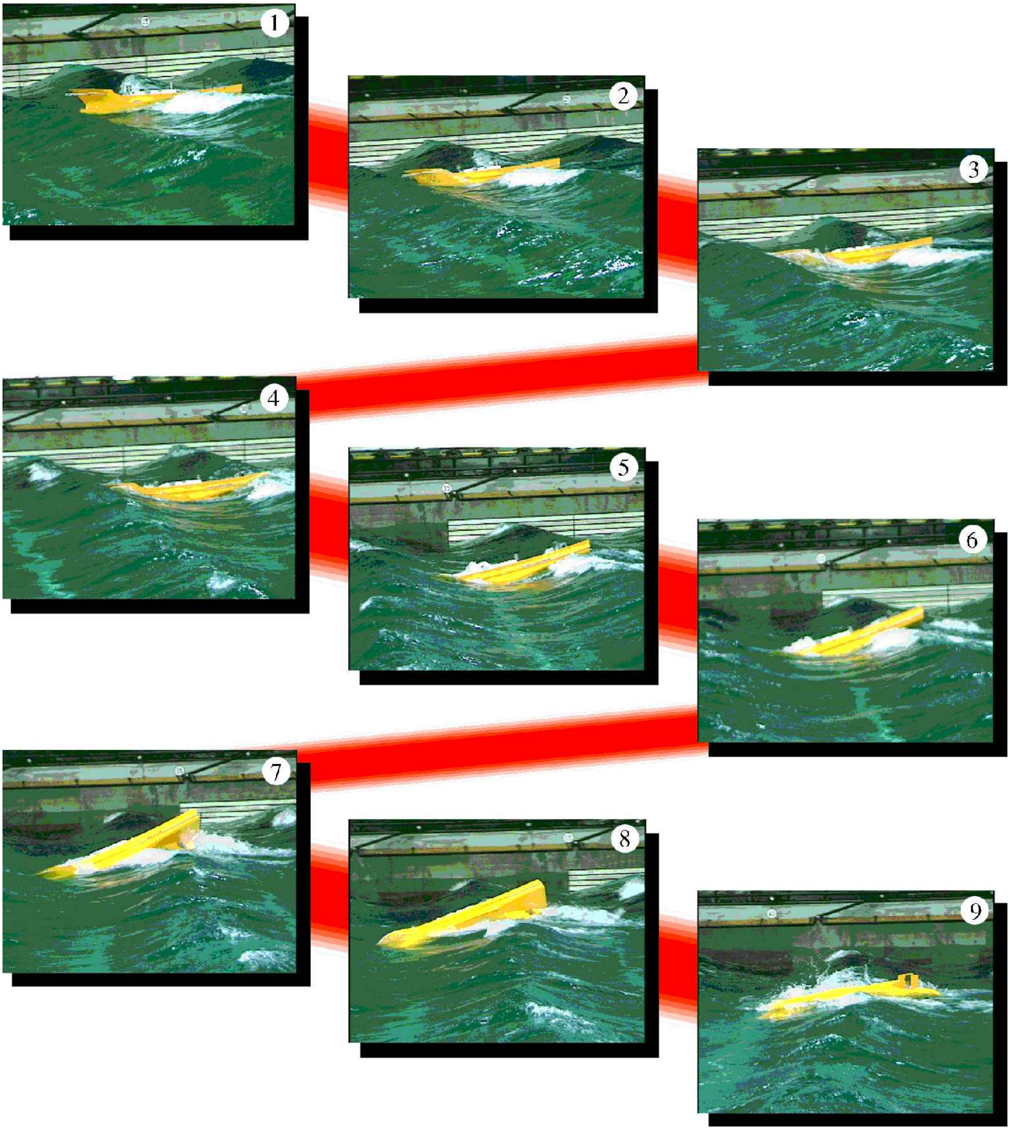

Figure 18. Photographs of capsizing due to plough-in for the 80 GT purse seiner with wave steepness of 1/8.8, wavelength-to-ship length ratio of 1.408, autopilot course of −10° and nominal Froude number of 0.46.

Then, substituting equation (4.1) into the differentiation of equations (A 2) and (A 3) with respect to time, we obtain

$$\dot{A} = -\frac{1}{\hat{\omega}}[\hat{\omega}^2\phi - 2\alpha\dot{\phi} - \omega_\phi^2(1 + M\cos 2\hat{\omega}t)\phi - \omega_\phi^2\beta\phi^3 + \gamma k\zeta_{\mathrm{w}}\omega_\phi^2 \sin\chi \sin 2\hat{\omega}t]\sin(\hat{\omega}t - \varepsilon), \tag{A 4}$$

$$\dot{\varepsilon} = \hat{\omega} + \frac{1}{\hat{\omega}A^2}[-A^2\hat{\omega}^2\sin^2(\hat{\omega}t - \varepsilon) + A\cos(\hat{\omega}t - \varepsilon) \times \{-2\alpha\dot{\phi} - \omega_\phi^2(1 + M\cos 2\hat{\omega}t)\phi - \omega_\phi^2\beta\phi^3 + \gamma k\zeta_{\mathrm{w}}\omega_\phi^2\sin\chi\sin 2\hat{\omega}t\}]. \tag{A 5}$$

PHILOSOPHICAL TRANSACTIONS OF THE ROYAL SOCIETY A MATHEMATICAL, PHYSICAL & ENGINEERING SCIENCES

Substituting equations (4.2) and (A 1) into equations (A4) and (A5) and averaging them over one period $T = 2\pi/\hat{\omega}$, we obtain equations (4.3) and (4.4). It is noteworthy here that the contribution from the exciting term mathematically disappears.

References

Ananiev, D. M. 1966 On surf-riding in following seas. *T. Krylov Soc.* **13**, 169–176. (In Russian.)

Dand, I. 1996 Directional instability and safety of high speed marine vehicles. In *Proc. 5th Int. Conf. on High Speed Marine Craft*, no. 17. Bergen: Norske Sivilingeniørers Forening.

Davidson, K. S. M. 1948 A note on the steering of ships in following sea. In *Proc. 7th Int. Conf. of Applied Mechanics, London*, pp. 554–556.

Hamamoto, M., Umeda, N., Matsuda, A. & Sera, W. 1995 Analyses on low cycle resonance in astern seas. *J. Soc. Naval Architects Japan* **177**, 197–206.

Hamamoto, M., Enomoto, T., Sera, W., Panjaitan, J. P., Ito, H., Takaishi, Y., Kan, M., Haraguchi, T. & Fujiwara, T. 1996 Model experiments of ship capsize in astern seas. 2nd report. *J. Soc. Naval Architects Japan* **179**, 77–87.

Kerwin, J. E. 1955 Notes on rolling in longitudinal waves. *Int. Shipbuilding Progr.* **2**, 597–614.

Makov, Y. 1969 Some results of theoretical analysis of surf-riding in following seas. *T. Krylov Soc.* **126**, 124–128. (In Russian.)

Matsuda, A., Umeda, N. & Suzuki, S. 1997 Vertical motions of a ship running in following and quartering seas. *J. Kansai Soc. Naval Architects* **227**, 47–55. (In Japanese.)

Motora, S., Fujino, M. & Fuwa, T. 1982 On the mechanism of broaching-to phenomena. In *Proc. 2nd Int. Conf. on Stability of Ships and Ocean Vehicles*, pp. 535–550. Tokyo: Society of Naval Architects of Japan.

Oakley, O. H., Paulling, J. R. & Wood, P. D. 1974 Ship motions and capsizing in astern seas. In *Proc. 10th Naval Hydrodynamics Symp.*, paper no. IV-1. Cambridge, MA: MIT Press.

Renilson, M. R. & Anderson, V. 1997 Deck diving of catamarans in following seas. In *Proc. 4th Int. Conf. on Fast Sea Transportation, Sydney*, pp. 463–469.

Sadakane, H. 1986 A criterion for ship capsize in beam seas. In *Proc. 3rd Int. Conf. on Stability of Ships and Ocean Vehicles, Gdansk*, vol. 1, pp. 119–124.

Spyrou, K. J. 1995 Surf-riding, yaw instability and large heeling of ships in following/quartering seas. *Schiffstechnik* **42**, 103–112.

Spyrou, K. J. 1997 Dynamic instability in quartering seas. Part III. Nonlinear effects on periodic motions. *J. Ship Res.* **41**, 210–223.

Taguchi, H. & Kan, M. 1992 Effects of the variation of stability on fractal capsize boundaries of a ship. *T. West Japan Soc. Naval Architects* **84**, 107–120. (In Japanese.)

Thompson, J. M. T. 1990 Transient basins: a new tool for designing ships against capsize. In *Dynamics of marine vehicles and structures in waves* (ed. W. G. Price, P. Temarel & A. J. Keane), pp. 325–331. Elsevier.

Thompson, J. M. T. 1997 Designing against capsize in beam seas: recent advances and new insights. *Appl. Mech. Rev.* **50**, 307–325.

Umeda, N. 1983 On the surf-riding. *J. Soc. Naval Architects Japan* **152**, 219–228. (In Japanese.)

Umeda, N. 1999 Nonlinear dynamics of ship capsize due to broaching in following and quartering seas. *J. Mar. Sci. Technol.* **4**, 16–26.

Umeda, N. & Kohyama, T. 1990 Surf-riding of a ship in regular seas. *J. Kansai Soc. Naval Architects* **213**, 63–74. (In Japanese.)

Umeda, N. & Renilson, M. R. 1992 Broaching—a dynamic behaviour of a vessel in following seas. In *Manoeuvring and control of marine craft* (ed. P. A. Wilson), pp. 533–543. Southampton: Computational Mechanics.

Umeda, N. & Vassalos, D. 1996 Nonlinear periodic motions of a ship running in following/quartering seas. *J. Soc. Naval Architects Japan* **179**, 89–101.

Umeda, N., Hamamoto, M., Takaishi, Y., Chiba, Y., Sera, W., Suzuki, S., Spyrou, K. J. & Watanabe, K. 1995*a* Model experiments of ship capsize in astern seas. *J. Soc. Naval Architects Japan* **177**, 207–217.

Umeda, N., Yamakoshi, Y. & Suzuki, S. 1995*b* Experimental study for wave forces on a ship running in quartering seas with very low encounter frequency. In *Proc. Int. Symp. on Ship Safety in a Seaway*, vol. 1, no. 14. Kaliningrad: Kaliningrad State Technical University Press.

Umeda, N., Vassalos, D. & Hamamoto, M. 1997 Prediction of ship capsize due to broaching in following/quartering seas. In *Proc. 6th Int. Conf. on Stability of Ships and Ocean Vehicles, Varna*, vol. 1, pp. 45–54.

Umeda, N., Matsuda, A., Hamamoto, M. & Suzuki, S. 1999 Stability assessment for intact ships in the light of model experiments. *J. Mar. Sci. Technol.* **4**, 45–57.

Wellicome, J. 1975 An analytical study of the mechanism of capsizing. In *Proc. Int. Conf. on Stability of Ships and Ocean Vehicles*, paper no. 3.1. Glasgow: University of Strathclyde Press.

Yamakoshi, Y., Takaishi, Y., Kan, M., Yoshino, Y. & Tsuchiya, T. 1982 Model experiments on capsize of fishing boats in waves. In *Proc. 2nd Int. Conf. on Stability of Ships and Ocean Vehicles*, pp. 199–214. Tokyo: Society of Naval Architects of Japan.